Overcoming organic and nitrogen overload in thermophilic anaerobic digestion of pig slurry by coupling a microbial electrolysis cell

Míriam Cerrillo[1], Marc Viñas[1], August Bonmatí[1*].

[1] IRTA. GIRO Joint Research Unit IRTA-UPC. Torre Marimon. E-08140, Caldes de Montbui, Barcelona (Spain).

e-mail addresses: miriam.cerrillo@irta.cat (M. Cerrillo); marc.vinas@irta.cat (M. Viñas); august.bonmati@irta.cat (A. Bonmatí).

ABSTRACT

The combination of the anaerobic digestion (AD) process with a microbial electrolysis cell (MEC) coupled to an ammonia stripping unit as a post-treatment was assessed both in series operation, to improve the quality of the effluent, and in loop configuration recirculating the effluent, to increase the AD robustness. The MEC allowed maintaining the chemical oxygen demand removal of the whole system of 46±5% despite the AD destabilization after doubling the organic and nitrogen loads, while recovering 40±3% of ammonia. The AD-MEC system, in loop configuration, helped to recover the AD (55% increase in methane productivity) and attained a more stable and robust operation. The microbial population assessment revealed an enhancement of AD methanogenic archaea numbers and a shift in eubacterial population. The AD-MEC combined system is a promising strategy for stabilizing AD against organic and nitrogen overloads, while improving the quality of the effluent and recovering nutrients for their reutilization.

Keywords

Microbial electrolysis cell (MEC), Thermophilic Anaerobic digestion, System stability, Ammonia recovery, Inhibition phenomenon.

* Corresponding author. Address: IRTA, GIRO Joint Research Unit IRTA-UPC, Torre Marimon, ctra. C-59, km 12,1. E-08140 Caldes de Montbui, Barcelona, Spain. Tel.: +34 902 789 449; Fax. +34 938 650 954.

1. Introduction

Anaerobic digestion (AD) of livestock manure and other wastes results in organic matter stabilization and biogas production, a biofuel containing mainly methane and carbon dioxide that can be used in power generation systems to obtain heat and electricity. This energy recovering technology is nowadays widely used to treat various kinds of wastes (Angenent et al., 2004). AD process is complex, since it involves many different groups of microorganisms, especially methanogens, that are particularly sensitive to organic overloads and diverse substances that may be present in the waste stream such as ammonia (Angelidaki and Ahring, 1993; Yenigün and Demirel, 2013). AD can mainly take place at two different ranges of temperatures, either mesophilic (25-40 ºC) or thermophilic (45-60 ºC). The later one is more favourable to obtain a high digestion rate, since high loading rates or short retention times can be applied, due to higher growth rates of bacteria at higher temperatures. Moreover, improved solids settling and destruction of microbial pathogens is attained (Angelidaki and Ahring, 1994). On the other hand, thermophilic AD has a lower process stability than mesophilic AD, it being more sensitive to high ammonia concentrations since free ammonia (NH_3), the active component causing ammonia inhibition, increases with an increase in pH and temperature (Angelidaki and Ahring, 1994). Reactor upset will be indicated by a reduction in biogas production and/or biogas methane content, and the accumulation of volatile fatty acids (VFA) that may lead to reactor failure (Chen et al., 2008). At a microbiology level, and due to the complex interdependence of microbial activities for the adequate functionality of anaerobic bioreactors, the genetic expression of *mcr*A, which encodes the α subunit of methyl coenzyme M reductase –the enzyme that catalyses the final step in methanogenesis–, has been proposed as a parameter to monitor the process performance (Alvarado et al., 2014; Morris et al., 2013).

Besides monitoring the AD process by means of CH_4 production, it is interesting to explore new technologies that can help AD to maintain effluent quality within the desired limits despite AD failure. So far, different strategies for stabilizing AD reactors under high organic loading rates and for controlling ammonia toxicity have been evaluated, ranging from the more classical approaches, such as co-digestion with carbon-rich substrates to equilibrate the carbon to nitrogen ratio (Chiu et al., 2013), introduction of adaptation periods (Borja et al., 1996), reduction of ammonia content of the substrates by air stripping (Bonmatí and Flotats, 2003; Laureni et al., 2013), or dilution of the substrates (Hejnfelt and Angelidaki, 2009); to more innovative ones, such as the use of an electrochemical system aimed at NH_4^+ extraction coupled to an upflow anaerobic sludge blanket (UASB) in the recirculation loop to help control ammonia toxicity with high nitrogen loading conditions (Desloover et al., 2014).

An alternative to these techniques is the use of bioelectrochemical systems (BES) in combination with an AD process. BESs are bioreactors that use microorganisms attached to one or both electrode(s) in order to catalyse oxidation and/or reduction reactions. These systems are also useful for recovering nutrients, such as ammonium (Sotres et al., 2015a). BESs have proven to be useful as post-treatment for anaerobic digesters in order to reduce organic matter content and recover ammonium (Cerrillo et al., 2016). Different AD-BES configurations have been previously studied, mainly aimed to improve biogas production in the AD (Tartakovsky et al., 2011; Zhang and Angelidaki, 2015). But more research in terms of combined system behaviour against factors that may destabilise the AD process is needed, as well as a more global approach of the AD-BES system integrating stabilization of the process, microbial community stability, improvement of the quality of the effluent, and nutrient recovery.

Since the effluent of a BES is expected to have a lower content of organic matter and ammonium, a combined AD-BES system with a recirculation loop between both components may offer some advantages in order to increase the stability of the system, mainly improving its resistance against organic and nitrogen overloads. The combination of BES with AD, as a system to reduce ammonia inhibition, has been previously demonstrated using a submersible microbial desalination cell fed with synthetic wastewater, although in that case the BES was not exploited to reduce organic matter content (Zhang and Angelidaki, 2015). On the other hand, although combined AD-BES systems have been tested against strong perturbations (Weld and Singh, 2011), the effect of stress on microbial synergies (eubacterial and archaeal communities) is scarcely known, especially on methanogenic archaea and their evolution when operating in a coupled system under inhibited and recovered stages.

The main aim of this study is to assess the combination of the AD process with a microbial electrolysis cell (MEC) both in series operation, as a system to improve the effluent quality, and in loop configuration to recirculate the effluent, as a technique to increase the stability and robustness of the AD process, while recovering ammonia with a stripping and absorption unit. Furthermore, microbial community dynamics have been assessed in both reactors to understand the reactor set-up effects, as well as microbial resilience at different operational conditions, even under an inhibited AD operation.

2. Materials and methods

2.1 Experimental set-up

A lab-scale continuous stirred tank reactor (CSTR) was used to study its performance when treating pig slurry at a thermophilic temperature range. The anaerobic digester (AD) consisted of a cylindrical glass reactor (25 cm diameter) with a 4 L working volume. The digester was fitted with a heat jacket with hot water circulating to keep the

temperature at 55 ºC. Thermophilic conditions were chosen as AD is more sensitive to the presence of inhibitors such as ammonia at this range of temperature. A temperature probe was fitted into de reactor lid for temperature monitoring. Continuous mixing was also supplied using an overhead stirrer. A gas counter was used to measure biogas production (μFlow, Bioprocess Control AB, Sweden). The digester was initially inoculated with 2,550 mL (64% of the AD volume) of the effluent of another lab scale thermophilic AD fed with sewage sludge from a wastewater treatment plant.

A two chamber cell BES reactor described elsewhere (Cerrillo et al., 2016) which had been previously operated in MEC mode with digested pig slurry was used for the experiments. The anode was a carbon felt (dimensions: 14 x 12 cm; thickness: 3.18 mm; Alfa Aesar GmbH and Co KG, Karlsruhe, Germany); and a 304 stainless steel mesh was used as cathode (dimensions: 14 x 12 cm; mesh width: 150 μm; wire thickness: 112 μm; Feval Filtros, Spain). Both compartments (0.5 L each one) were separated by a cation exchange membrane (CEM, dimensions: 14 x 12 cm; Ultrex CMI-7000, Membranes International Inc., Ringwood, NJ, USA). A potentiostat (VSP, Bio-Logic, Grenoble, France) was used to poise the anode (working electrode) potential at 0 mV in a three electrode mode, with an Ag/AgCl reference electrode (Bioanalytical Systems, Inc., USA) inserted in the anode compartment (+197 mV vs. standard hydrogen electrode, SHE). All potential values in this paper are referred to SHE. The potentiostat was connected to a personal computer which recorded electrode potentials and current, every 5 min, using EC-Lab software (Bio-Logic, Grenoble, France).

A stripping and absorption system was used to recover the ammonium transferred from the anode to the cathode compartment. It consisted of two glass columns (70 cm height; 7 cm $Ø_{external}$; 5.5 cm $Ø_{internal}$) filled with glass rings (5-7 mm length). The cathode effluent was initially conducted to the top of the stripping column, and later circulated

through the filling towards the bottom while air was pumped in the opposite direction. The air leaving the top of the column was directed to the absorption column, which was filled with an acidic solution (H_2SO_4, 10% v/v). Figure 1 shows the scheme of the complete AD-MEC-Stripping/Absorption combined system.

2.2 Reactors operation

The AD was fed in a continuous mode with raw pig slurry from a farm in Vila-Sana (Lleida, Spain) with a hydraulic retention time (HRT) of 10 days. The pig slurry was diluted with tap water to obtain the desired organic load; the characteristics of the influent used can be seen in Table 1. The reactor was operated during 336 days in 5 different phases (Table 2). In Phase 1, the organic loading rate (OLR) was of 3.02±0.60 kg_{COD} m^{-3} day^{-1} and the nitrogen loading rate (NLR) was of 0.17±0.03 kg_N m^{-3} day^{-1}. In Phase 2, the previous OLR and NLR were doubled (6.25±1.05 kg_{COD} m^{-3} day^{-1}; 0.34±0.06 kg_N m^{-3} day^{-1}) to evaluate the stability of the reactor with an organic overload, and the AD effluent was used to feed the MEC from day 160, after 4 HRT, as a polishing step and a system to recover ammonia. In Phases 3, 4 and 5 a recirculation loop between the AD and the MEC was introduced, with 25%, 50% and 75% of feed flow rate recirculation, respectively, so as to study the effectiveness of this recirculation as an AD stabilization strategy. As an effect of the recirculation, the real HRT in the AD decreased from 10 days to 8, 6.7 and 5 days (recirculation flow rates of 25, 50 and 75% of the fed flow rate, respectively). Each phase was maintained at least for 4 HRT to ensure a stable operation. For each experimental condition, specific methane productivity rate (m^3_{CH4} m^{-3} d^{-1}) and chemical oxygen demand (COD) removal efficiencies were used as control parameters, as well as biogas composition, alkalinity, $N\text{-}NH_4^+$ and VFA concentrations in the effluent, samples which were taken once a week.

With regards to the MEC, the digested pig slurry obtained from the AD was later used as feed for the anode compartment, previously filtering it in batches through a 125 μm stainless steel sieve. Filtering removed an average of 5% of the AD influent COD, and this amount was included in the calculations of COD removal efficiency. Table 2 shows the average OLR and NLR for each Phase. The feeding solution for the cathode chamber contained (in deionised water) NaCl 0.1 g L^{-1}. The solutions of both the anode and the cathode compartment were fed in continuous mode at 14 mL h^{-1} and mixed recirculating them with an external pump. The stripping and absorption system was operated in Phases 2 and 3 to prove the feasibility of the full combined system. The MEC was operated at room temperature during the entire assay (~ 23 ºC). Samples were taken 3 times a week to analyse pH and N-NH_4^+ in the anode and cathode effluents and the acidic solution of the absorption column, besides COD and VFA of the anode effluent.

2.3. Analytical methods and calculations

Kjeldahl nitrogen (NTK), ammonium (N-NH_4^+), alkalinity, chemical oxygen demand (COD), total solids (TS), volatile solids (VS), volatile fatty acids (VFAs), biogas composition (N_2, CH_4, CO_2) and pH were determined according to methods previously described (Cerrillo et al., 2016). Partial alkalinity (PA, titration from the original pH sample to pH 5.75, an alkalinity which corresponds roughly to bicarbonate alkalinity) and total alkalinity (titration to pH 4.3) were determined to obtain intermediate alkalinity (IA, titration from 5.75 to 4.3, approximately the VFA alkalinity) (Ripley et al., 1986). The IA:TA ratio was used as a tool to monitor anaerobic digestion, considering that the process was stable when the IA:TA was below 0.3.

Free ammonia concentration was calculated from the equilibrium relationship:

$$[NH_3] = \frac{[T - NH_3]}{\left(1 + \frac{H^+}{k_a}\right)}$$

where $[NH_3]$ and $[T\text{-}NH_3]$ are respectively the free and the total ammonia (NTK) concentrations, and k_a the dissociation constant with a value of $38.3 \cdot 10^{-10}$ at 55 °C.

The current density (A m^{-2}) of the MEC was calculated as the quotient between the intensity recorded by the potentiostat (A) and the area of the anode (m^2). Ammonium and COD removal efficiencies in the MEC were calculated as the ratio of the difference between the anode influent and effluent concentrations and the influent concentration.

2.4. Microbial community analysis

To better understand the results obtained, the bacterial communities present in the AD at the end of each Phase from 1 to 5, attached to the anode of the MEC at the beginning and at the end of the experiments, were analyzed by culture-independent molecular techniques, such as quantitative real-time polymerase chain reaction (qPCR) and high throughput DNA sequencing (MiSeq, Illumina).

2.4.1 Quantitative PCR assay (qPCR)

Gene copy numbers of eubacterial *16S rRNA* gene and *mcrA* gene (methanogenic archaeal methyl coenzyme-M reductase) were quantified by means of quantitative real-time PCR (qPCR). Total DNA was extracted in triplicate from known weights of each sample with the PowerSoil® DNA Isolation Kit (MoBio Laboratories Inc., Carlsbad, CA, USA), following the manufacturer's instructions. Each sample was analyzed in triplicate by means of the three independent DNA extracts. The analysis was carried out by using Brilliant II SYBR Green qPCR Master Mix (Stratagene, La Jolla, CA, USA) in a Real-Time PCR System Mx3000P (Stratagene) operated with the following protocol: 10 min at 95 ºC, followed by 40 cycles of denaturation at 95 ºC for 30 s, annealing for 30 s at 55 ºC and 54 ºC (for *16S rRNA* and *mcrA* gene, respectively), extension at 72 ºC for 45 s, and fluorescence capture at 80 ºC for 30 s and 15 s (for *16S rRNA* and *mcrA* gene, respectively). The specificity of PCR amplification was determined by observations on a melting curve and gel electrophoresis

profile. A melting curve analysis, to detect the presence of primer dimmers, was performed after the final extension, increasing the temperature from 55 to 95 ºC at heating rates of 0.5 ºC each 10 s. Image capture was performed at 80 ºC to exclude fluorescence from the amplification of primer dimmers. Each reaction was performed in 10 µL volumes containing 1 µL of DNA template, 200 nmol L^{-1} of each *16S rRNA* primer, 600 nmol L^{-1} of each *mcrA* primer, 5 µL of the ready reaction mix, and 30 nmol L^{-1} of ROX reference dye. The primer set for eubacterial population was 341F (5′-CCTACGGGAGGCAGCAG-3′) and 518R (5′-ATTACCGCGGCTGCTGG-3′). The primer set for archaeal *mcrA* gene was ME1F (5′-GCMATGCARATHGGWATGTC-3′) and ME3R (5′-TGTGTGAASCCKACDCCACC-3′); both primer pairs were purified by HPLC. The standard curves were performed with the following reference genes: a *16S rRNA* gene from *Desulfovibrio vulgaris* ssp. *vulgaris* ATCC 29579, and a *mcrA* gene fragment obtained from *Methanosarcina barkeri* DSM 800, both inserted in a TOPO TA vector (Invitrogen Ltd, Paisley, UK). All reference genes were quantified by NanoDrop 1000 (Thermo Scientific). Ten-fold serial dilutions of known copy numbers of the plasmid DNA, in the range of 10^2 to 10^9 copies for *16S rRNA* gene and in the range of 10 to 10^8 copies for *mcrA* gene, were subjected to a qPCR assay in duplicate to generate the standard curves. All results were processed by MxPro QPCR Software (Stratagene). The standard curve parameters of the qPCRs performed showed a high efficiency and were as follows (for 16S rRNA and mcrA, respectively): a slope of -3.407 and -3.591; a correlation coefficient of 0.999 and 0.998; and an efficiency of 97 and 90%.

2.4.2 High throughput DNA sequencing and data analysis

The same DNA extracted from the AD effluent and the anode of the MEC used for qPCR analysis was used for sequencing purposes. The specific steps of MiSeq analysis for eubacteria and archaea were done as follows. Massive bar-coded *16S rRNA* gene libraries targeting eubacterial region V1-V3 *16S rRNA* and archaeal region V3-V4 were sequenced

utilizing MiSeq equipment (Illumina, San Diego, CT, USA). Each DNA was amplified separately with both the *16S rRNA* eubacteria and archaea sets of primers. For eubacteria libraries the primer sets were 27F (5'-AGRGTTTGATCMTGGCTCAG–3') and 519R (5'-GTNTTACNGCGGCKGCTG-3'), while the archaeal sets of primers were 349F (5'-GYGCASCAGKCGMGAAW-3') and 806R (5'–GGACTACVSGGGTATCTAAT-3'). Sequencing was performed at MR DNA (www.mrdnalab.com, Shallowater, TX, USA) on a MiSeq instrument following the manufacturer's guidelines. The taxonomic assignment of obtained Operational Taxonomic Units (OTUs) was carried out by means of the Naïve Bayesian Classifier tool in the Ribosomal Database Project (RDP training set 14) (Wang et al., 2007). All data obtained from sequencing datasets were submitted to the Sequence Read Archive of the National Center for Biotechnology Information (NCBI, U.S.A) under study accession number SRP063053 for eubacterial and archaeal populations.

To evaluate the diversity of the samples, the number of OTUs, the inverted Simpson index, Shannon index, Goods coverage and Chao1 richness estimator were all calculated using the Mothur software v.1.34.4 (http://www.mothur.org) (Schloss et al., 2009). All the estimators were normalized to the lower number of reads from the different samples. A statistical correspondence analysis of MiSeq data was performed by means of the XLSTAT 2014 software (Addinsoft, Paris, France).

3. Results and discussion

3.1. Performance of the AD independent operation

After the start-up of the AD, in Phase 1 the COD removal efficiency increased from values in the range of 10-20% up to values in the range of 55-63% (Figure 2a), with COD effluent values in the range of 14.25–16.48 g kg^{-1}. When the OLR was doubled in Phase 2, the COD removal efficiency decreased down to values in the range of 20-28%, increasing the COD of the effluent up to 43.58 – 51.65 g kg^{-1}. During Phase 1, maximum methane

productivity was of 0.33 m^3 m^{-3} d^{-1}, increasing to 0.56 m^3 m^{-3} d^{-1} at the beginning of Phase 2 as a response to the increase in OLR (Figure 2b). Nevertheless, methane productivity dropped down in the following weeks and was of only 0.12 m^3 m^{-3} d^{-1} after 80 days of operation under these new conditions, representing a 63% decrease with respect to the previous phase, as a result of a severe inhibition due to the increase of OLR and NLR. This inhibition process can also be observed with the IA:TA ratio (Figure 2c) found to be in the range of 0.21-0.26 at the end of Phase 1 –well below the 0.30 limit for a stable operation– but increased up to 0.52 after the stress produced by the increase of the OLR and NLR. These results are in accordance with the VFA content (Figure 2d), as there was an increase in values, starting under 1000 mg_{COD} L^{-1} (585 mg_{acetic} L^{-1} and 175 $mg_{propionic}$ L^{-1}) at the end of Phase 1, and going up to a maximum of 17000 mg_{COD} L^{-1} in Phase 2, reaching values of 4808 mg_{acetic} L^{-1}, 1384 $mg_{propionic}$ L^{-1}, 794 $mg_{iso\text{-}butyric}$ L^{-1}, 1634 $mg_{n\text{-}butyric}$ L^{-1}, 838 $mg_{iso\text{-}valeric}$ L^{-1}, 686 $mg_{n\text{-}valeric}$ L^{-1} 137 $mg_{iso\text{-}caproic}$ L^{-1} and 924 $mg_{n\text{-}caproic}$ L^{-1}. This accumulation of VFA is a clear indication that the methanogenic population is inhibited, as well as of AD failure. Average values in each Phase (stable period) for COD removal efficiency, methane productivity, biogas composition, pH, alkalinity and IA:TA ratio are shown in Table 3.

Inhibition of AD by ammonia has been long studied (Yenigün and Demirel, 2013). In one of these studies, cattle manure was used as the substrate in continuously fed thermophilic laboratory scale reactors, gradually administering NH_4Cl for adaptation while the pH was kept constant. The first signs of inhibition occurred at a total ammonia nitrogen (TAN) concentration of 4000 mg L^{-1} –i.e. free ammonia nitrogen + ammonium nitrogen–, corresponding to 900 mg L^{-1} of free ammonia nitrogen (FAN). Process instability due to the presence of ammonia led to VFA accumulation, which lowered the pH. As a result, the decreased FAN concentration eventually resulted in a stable, though lowered, methane yield, called by the authors the ‘inhibited steady state’ (Angelidaki and Ahring, 1993).

Another study investigated the digestion of swine manure in a laboratory scale batch and CSTRs –again in thermophilic conditions–, and concluded that a threshold of 1100 mg L^{-1} FAN concentration was required for introducing inhibition (Hansen et al., 1998). The values in the present study for FAN are quite below the inhibitory values indicated in those works, except at the beginning of Phase 2 (Figure 2e). The increase in NLR, summed to an increase in the pH of the reactor, raised the FAN concentration up to 960 mg L^{-1}. From then on, the first signs of inhibition were shown, with a decrease in COD removal efficiency and methane productivity and VFA accumulation. Later, this VFA accumulation produced a decrease in pH and in the FAN concentration, even if the reactor did not show signs of recovery. This fact can be explained because the levels of VFA, especially for propionic acid, remained high and could inhibit the activity of methanogens. Although VFA levels for which an AD reactor can show inhibition may differ from one digester to another, Wang et al. (2009) reported that acetic acid and butyric acid concentrations of 2400 and 1800 mg L^{-1}, respectively, resulted in no significant inhibition of the activity of methanogens, while a propionic acid concentration of 900 mg L^{-1} resulted in their significant inhibition. The VFA concentration of the AD was above these values, so the observed inhibition was probably produced by the combination of high ammonia and VFA concentrations.

3.2. Performance of the AD-MEC combined system in series operation

The MEC was fed with the effluent of the AD during Phase 2, as a polishing step and a way to buffer the malfunction period of the AD. The average COD removal efficiency achieved in the MEC was of 25±8% (Table 3), resulting in an effluent COD of 31.48±4.52 g kg^{-1} and a total COD removal efficiency of the combined system of 46±5%. The VFA were reduced at the effluent to a range of 6418-8804 mg_{COD} L^{-1}, maintaining acetic and propionic under 2000 and 1000 mg L^{-1}, respectively (Figure 3c). Furthermore, concomitant to COD removal, an average of 2.01±0.63 A m^{-2} were produced (Figure 3a) and 40±3% of the

ammonia was transferred from the anode to the cathode compartment (12.97±2.04 g N-NH_4^+ d^{-1} m^{-2}) (Figure 3b). Those values were equivalent to the obtained in a recent work with an electrochemical system in the recirculation loop of an UASB (Desloover et al., 2014) but lower to the 86 g N-NH_4^+ d^{-1} m^{-2} obtained with a submersible microbial desalination cell fed with synthetic solution (Zhang and Angelidaki, 2015). With the stripping and absorption step, up to 37% of the ammonia of the anode compartment influent was recovered in the acidic solution. Such high recovery was achieved thanks to the high cathode effluent pH (11.83±0.60), due to charge and cation transfer between the anode and cathode compartments (Cerrillo et al., 2016) while the pH of the anode effluent remained neutral (7.03±0.07).

3.3. Performance of the AD-MEC combined system with recirculation loop

When the recirculation loop between the AD and the MEC was established, starting with a volume of 25% of the feed flow rate in Phase 3, a clear recovery of the AD was observed. After a period of 4 HRT, the COD removal efficiency reached up to 38% and methane productivity increased up to 0.35 m^3 m^{-3} d^{-1}, equalling the productivity obtained before the inhibition (Figure 2b). The IA:TA ratio also showed an improvement, decreasing from 0.56 to 0.46, parallel to the VFA decrease to 11740 mg_{COD} L^{-1} (4477 mg_{acetic} L^{-1} and 1088 $mg_{propionic}$ L^{-1}). In these conditions, the MEC achieved a COD and ammonium removal efficiency of 28±7% and 31±5%, respectively (Table 3). The AD-MEC combined system achieved a COD removal efficiency of 51±7%, resulting in an effluent COD of 28.88±2.69 g kg^{-1}.

When the recirculation between MEC and AD was increased to 50% of the feed flow rate (Phase 4), the COD removal of the AD stabilized at an average of 35±4% and a methane productivity of 0.42±0.05 m^3 m^{-3} d^{-1}. This productivity represented a 55% increase with respect to the one obtained before the inhibition, when the OLR was a half, and a 7

fold increase with respect to inhibited state in Phase 2 (Table 3). The IA:TA ratio showed an improvement at the end of Phase 4, decreasing to a value of 0.38, since VFA were stabilized at around 8500 mg_{COD} L^{-1} (3200 mg_{acetic} L^{-1} and 1000 $mg_{propionic}$ L^{-1}). The MEC achieved a COD and ammonium removal efficiency of 30±11% and 22±5%, respectively (Table 3). This way the AD-MEC combined system achieved an overall COD removal efficiency of 59±7%, with an effluent COD of 28.10±6.04 g kg^{-1}.

Finally, in Phase 5 the recirculation volume was increased up to 75% of the feed flow rate. This time the AD showed the highest COD removal efficiency from the three recirculation phases, with an average of 42±3% (Figure 2). Methane productivity and IA:TA ratio were similar on average to the previous phase (0.38±0.06 m^3 m^{-3} d^{-1} and 0.42±0.02, respectively), although with a slight tendency to worsen, which can be due to the biomass wash out produced by an excess in recirculation volume. VFA were stabilized in a range of 3800 – 4150 mg_{COD} L^{-1} (2750 mg_{acetic} L^{-1} and 750 $mg_{propionic}$ L^{-1}). The MEC achieved a COD and ammonium removal efficiency of 20±7% and 17±5%, respectively (Table 3). The AD-MEC combined system achieved a COD removal efficiency of 56±7%, resulting in an effluent COD of 27.27±3.67 g kg^{-1}.

From these results it can be seen that MEC removal efficiencies, both for COD and for ammonium, decreased at the same time that the AD recovered its performance, and the average current density produced in Phase 5 represented only 42% of the average current density of Phase 2. This behaviour can be explained because the AD effluent decreased the COD concentration when the recirculation loop was connected, so less organic matter was available for degradation by microorganism in the MEC (especially acetate) and less electrical intensity was produced, reducing also ammonium transport between anode and cathode. In return, removal efficiencies of the MEC were higher during the inhibition period of the AD, counterbalancing its poor performance.

The beneficial effect of the recirculation loop between the MEC and the AD can be due to different aspects. In the first place, the MEC contributes to decrease ammonia inhibition in the AD in two ways: by ammonium removal of the effluent, since it transfers from the anode to the cathode compartment, decreasing its concentration in a range of 17-31%; and by slightly decreasing the pH of the AD, and therefore the FAN level, as proton accumulation is induced in the anode compartment of the MEC due to charge and cation transport to the cathode. In the second place, the recirculation of the MEC effluent reduces also the organic load of the AD, since the MEC removes between 20 to 30% of the remaining COD. And finally, the robustness and stability of the AD may be increased thanks to the biomass connection between both reactors (section 3.4.). A recent work, focused on ammonium recovery with a desalination cell to overcome AD inhibition achieved a 40.8% recovery of ammonium and helped to gradually increase methane productivity back to 83%, compared to the control, 55 days after the inhibition of the AD (Zhang and Angelidaki, 2015). In that case, synthetic wastewater was used, and the inhibition of the AD was produced only increasing the NLR; while in this work, a more complex and realistic inhibition process has been induced, increasing both OLR and NLR. Furthermore, the set up proposed by Zhang and Angelidaki (2015) does not make the most of the BES in order to reduce the COD of the AD effluent. Hence a more integrated approach is presented in this study since not just the recovery of AD, after its inhibition, is achieved, but the COD concentration in the effluent is kept low.

3.4. Microbial community assessment

The microbial community structure of the AD at the end of each Phase, as well as the biofilm developed on the carbon felt (anode) of the MEC reactor, at the start and at the end of the assays, were characterized by means of qPCR technique and sequenced by MiSeq.

3.4.1 Quantitative analysis by qPCR

Figure 4 shows qPCR results for all the samples. The number of bacterial *16S* rRNA gene copies g^{-1} in the AD sample at the end of Phase 1 was of $8.42 \cdot 10^9$, and slightly oscillated throughout the different phases, with a maximum of $1.40 \cdot 10^{10}$ (a 1.7 fold increase) at the end of Phase 3. The *mcrA* gene copy numbers quantified by qPCR revealed that the initial abundance of $4.57 \cdot 10^7$ copy numbers g^{-1} at the end of Phase 1, decreased gradually to a minimum at the end of Phase 4 ($9.55 \cdot 10^6$ copy numbers g^{-1}). The sample taken at the end of Phase 5 showed a level of *mcr*A copy numbers similar to the one obtained in Phase 2 ($2.19 \cdot 10^7$ copy numbers g^{-1}). These values, including those corresponding to the inhibited state, are higher than those obtained in other studies, which quantified *mcrA* copies in different anaerobic digesters in a range of $1.04 \cdot 10^6$-$3.95 \cdot 10^6$ copy numbers mL^{-1} (Steinberg and Regan, 2009). The evolution of archaea population was found to be in great correlation with the operational parameters described in the previous sections, although a delay in the response was observed. The reduction in *mcrA* copy numbers under inhibited state, although working with lower ammonium concentrations, is similar to a previous study. qPCR in that work revealed that *mcrA* copy number decreased by one order of magnitude in the treatment with large amount of ammonium (10 g NH_4^+-N L^{-1}) but did not change much with treatments with lower NH_4^+-N content (3 and 7 g NH_4^+-N L^{-1}) compared to the control (Zhang et al., 2014). The ratio between archaea and eubacteria in the AD is under 1% in all cases, in spite of the importance of methanogenic archaea in AD, which is in agreement with previous studies (Sundberg et al., 2013). Regarding the MEC, an increase of an order of magnitude in *mcrA* copy numbers –at late stages– in the final sample, with respect to the initial one is produced, as a result of allochthonous methanogenic archaea coming from the AD. The same increase was also observed in bacterial *16S* rRNA gene copies.

3.4.2 MiSeq sequencing of total eubacteria and archaea, biodiversity and correspondence analysis

The reads obtained for bacteria and archaeal communities in each sample are shown in Table 4. Figure 5a shows that the dominant eubacterial *phyla* identified in the anode biofilm sample of the MEC at the start of the assay was *Bacteroidetes (31%),* followed by *Proteobacteria (21%),* while at the end of the assay a clear enrichment in the *Firmicutes* group took place, representing 66% of the relative abundance. These three phyla have been identified in previous studies in BES (Bonmatí et al., 2013; Sotres et al., 2015b). At family level, results in Figure 5b revealed the dominance of *Desulfuromonadaceae* (17%), *Anaerolineaceae* (16%) and *Flavobacteriaceae* (13%) at the start of the assay, and a clear enrichment in *Clostridiaceae* (43%) and Peptostreptococcaceae (14%) once the recirculation loop with the AD was established.

Regarding the samples of the AD effluent, *Firmicutes phylum* (63%) was de predominant one at the end of Phase 1, followed by *Proteobacteria* (28%). A previous study, performed also in a thermophilic AD running on swine manure by means of 454-pyrosequencing technology, also found that the *Firmicutes* phylum was the predominant one, representing 72.2% of the 16S rRNA gene sequences (Tuan et al., 2014). At the end of Phase 2, whilst the reactor was inhibited, *Firmicutes* increased its relative abundance up to 75% and *Proteobacteria* decreased to 7%. Once the recirculation loop with the MEC was established, both *phyla* equilibrated their presence at the end of Phase 3 (41%) and *Proteobacteria* surpassed *Firmicutes* in Phase 4, while at the end of Phase 5 *Firmicutes* recovered its dominance (57%). This *phylum* has been also observed to be in domination in AD under ammonia inhibition in previous studies (Niu et al., 2013). Furthermore, *Firmicutes* showed an important increase in the MEC anode, as aforementioned, it being a clear example of population sharing between both systems. Indeed, 6 OTUs belonging to the

Firmicutes phylum, not detected in the initial MEC sample but present in the AD, increased in relative abundance in the final MEC sample after the AD-MEC combined operation (Table SI1). On the other hand, *Bacteroidetes,* the predominant *phylum* in the MEC anode at the beginning of the assays, increased its relative abundance in the AD from 4% to 32% once the recirculation loop was established, and until Phase 5. Coincidentally, 4 new OTUs belonging to the *Bacteroidetes phylum* showed up in the AD, once the recirculation loop was connected (Table SI2). The most abundant OTUs in the final MEC sample, three belonging to the *Firmicutes phylum* and one belonging to the *Bacteroidetes phylum*, were shared by the AD at the end of Phase 5 (Table SI3). At family level, *Pseudomonadaceae* (20%), *Thermodesulbobiaceae* (16%) and *Clostridiaceae* (15%) were the predominant ones at the end of Phase 1. At the end of Phase 2, during the inhibition phase, Clostridiaceae increased its relative abundance (20%) whith the other two families decreasing. *Peptostreptococcaceae* and *Ruminococcaceae* increased slightly their relative abundance, becoming the second and third most abundant families (14 and 11%, respectively). During Phase 3 and 4, with the recirculation loop established, *Pseudomonadaceae* showed an important increase, up to 40 and 44%, respectively, but suffered a sharp decrease at the end of Phase 5, and *Clostridiaceae*, after decreasing to 7% in Phase 3, recovered its initial relative abundance at the end of Phase 5. Finally, it is noteworthy to mention that possible syntrophic acetate-oxidizing bacteria (SAOB) OTUs, such as *Syntrophaceticus* or *Tepidanaerobacter*, were detected in the AD samples, showing higher relative abundances during Phases 1, 2 and 3 (0.60, 0.51 and 0.50, respectively) than in Phases 4 and 5 (0.19 and 0.32, respectively). The high concentration of ammonia in the reactor might be favouring syntrophic acetate oxidation (SAO) coupled to a hydrogenotrophic methanogenesis route, which consisting in the oxidation of methyl and carboxyl groups of acetate to CO_2, producing H_2, catalyzed by the SAOB (Hattori, 2008).

Correspondence analysis for eubacterial population indicated that initial biofilm from the MEC anode evolved during the recirculation phases, approaching the composition of the AD samples, although maintaining its own specific composition. AD samples from the recirculation phases (3, 4 and 5) clustered together, moving away from samples of the phases without recirculation (1 and 2) (Figure SI1a).

Regarding archaeal population, Figure 5c shows that the most abundant families in the anode of the MEC at the start of the experiments were *Methanomassiliicoccaceae* (37%), *Methanosarcinaceae* (20%), *Methanomicrobiaceae* (15%) and *Methanotrichaceae* (formerly known as *Methanosaetaceae*) (15%). The last family, of strictly acetotrophic methanogens, was clearly enriched at the end of the assays, the recirculation loop with the AD once established, achieving a relative abundance of 94%. The AD presented, at the end of Phase 1, a high dominance of the *Methanobacteriaceae* family (98%), hydrogenotrophic methanogens, dominance maintained throughout the inhibition of the reactor in Phase 2. The predominance of hydrogenotrophic methanogens could be favoured by the low HRT used in this study, since the difference in the specific growth rate between hydrogenotrophic methanogens and aceticlastic methanogens makes for a relatively short HRT to provide a more favourable environment for the first ones. Furthermore, it has been reported that *Methanobacteriaceae* became the dominant species when increasing ammonia levels in biogas reactors (Kim et al., 2014). The *Methanobacteriaceae* family was also the predominant one in a thermophilic AD running on swine manure (Tuan et al., 2014). The community of a mesophilic real scale AD fed with swine faeces was composed, up to 57.7%, of by *Methanobacteriales*, hydrogenotrophic methanogens also being the dominant methane producing archaea (more than 94% of methanogenic archaea of the reactor) (Zhu et al., 2011). Although a slight decrease in the *Methanobacteriaceae* family relative abundance was observed during Phase 3 and 4, the highest decrease was observed at the end of Phase 5

–up to 58%. In parallel with this decrease, an increase in *Methanotrichaceae* was observed, reaching up to 31% at the end of Phase 5, whilst also becoming the predominant archaea in the MEC anode, as aforementioned. An OTU shared by the MEC and the AD was the dominant one in the *Methanotrichaceae* family, either in the final MEC and the AD Phase 5 sample (Table SI4). This shift in population towards acetotrophic methanogens can be stimulated by more favourable conditions in the AD in subsequent phases, once the ammonia concentration in the AD is reduced and the inhibition is overcome. These results correlate quite well with the ones obtained by qPCR, indicating that the inhibition of the AD regarding methane productivity and AGV increase is detected before a change in archaeal population abundance and composition is observed. Although the changes in the total population of methanogens can be used as an indicator of the performance of the AD, methanogenesis inhibition is largely due to the repression of functional gene expression (Zhang et al., 2014) and a deep study at RNA level in this sense would help to better link community structures and digester functions. Correspondence analysis for archaea population showed that initial and final biofilm from the MEC anode were far more distant in composition than in the case of the eubacteria population, and there was not a clear approach to the composition of the AD samples. AD samples were all clustered together, appreciating that the phases without recirculation (1 and 2) were quite similar, while a slight evolution in the recirculation phases samples (3, 4 and 5) could be observed (Figure SI1b).

Regarding biodiversity, the inverted Simpson and Shannon indexes showed that the sample of the MEC at the start of the assays was the most diverse one, either for eubacteria (17.50 and 4.27, respectively) and for archaea (8.12 and 2.39, respectively) (Table 4). For the AD, biodiversity indexes for eubacteria showed that the values corresponding to Phase 2 decreased with respect to Phase 1, but the minimum values were detected at the end of Phase 4. In Phase 5, the diversity values were near to the initial values. The AD archaea

biodiversity increased over time, finishing Phase 5 with the highest values for the inverted Simpson (2.47) and Shannon (1.29). These results show that the AD diversity was increased by the parallel treatment of the substrate, and in spite of the stressful conditions in the reactor, the exchange with the MEC biomass seems to help to recover its biodiversity.

4. Conclusions

Coupling an inhibited AD in series, with a MEC and a stripping and absorption unit allowed for the maintenance of the effluent quality (COD removal and ammonia recovering of 46±5% and 40±3%, respectively). The AD-MEC system in loop configuration stabilised the AD after failure (55% increase in methane productivity) and enhanced methanogenic archaea recovery, concomitant to an AD biodiversity increase, while reducing it in the MEC biofilm. These results show that the AD-MEC combined system is a promising strategy to stabilize AD against organic and nitrogen overloads, while improving the quality of the effluent and recovering nutrients for their reutilization.

Acknowledgements

This research was funded by the Spanish Ministry of Economy and Competitiveness (INIA project RTA2012-00096-00-00). The first author was supported by a PhD grant from the Secretariat for Universities and Research of the Ministry of Economy and Knowledge of the Catalan Government (pre-doctoral grant 2013FI_B 00014).

Appendix A. Supplementary data

Supplementary data associated with this article can be found, in the online version, at XXX.

References

1. Alvarado, A., Montáñez, L., Palacio Molina, S.L., Oropeza, R., Luevanos Escareno, M.P., Balagurusamy, N. 2014. Microbial trophic interactions and mcrA gene expression in monitoring of anaerobic digesters. *Frontiers in Microbiology*, 5.

2. Angelidaki, I., Ahring, B.K. 1994. Anaerobic thermophilic digestion of manure at different ammonia loads: Effect of temperature. *Water Research*, 28(3), 727-731.

3. Angelidaki, I., Ahring, B.K. 1993. Thermophilic anaerobic digestion of livestock waste: the effect of ammonia. *Applied Microbiology and Biotechnology*, 38(4), 560-564.

4. Angenent, L.T., Karim, K., Al-Dahhan, M.H., Wrenn, B.A., Domíguez-Espinosa, R. 2004. Production of bioenergy and biochemicals from industrial and agricultural wastewater. *Trends in Biotechnology*, 22(9), 477-485.

5. Bonmatí, A., Flotats, X. 2003. Air stripping of ammonia from pig slurry: characterisation and feasibility as a pre- or post-treatment to mesophilic anaerobic digestion. *Waste Management*, 23(3), 261-272.

6. Bonmatí, A., Sotres, A., Mu, Y., Rozendal, R.A., Rabaey, K. 2013. Oxalate degradation in a bioelectrochemical system: Reactor performance and microbial community characterization. *Bioresource Technology*, 143(0), 147-153.

7. Borja, R., Sánchez, E., Weiland, P. 1996. Influence of ammonia concentration on thermophilic anaerobic digestion of cattle manure in upflow anaerobic sludge blanket (UASB) reactors. *Process Biochemistry*, 31(5), 477-483.

8. Cerrillo, M., Oliveras, J., Viñas, M., Bonmatí, A. 2016. Comparative assessment of raw and digested pig slurry treatment in bioelectrochemical systems. *Bioelectrochemistry*, 100, 69-78.

9. Chen, Y., Cheng, J.J., Creamer, K.S. 2008. Inhibition of anaerobic digestion process: A review. *Bioresource Technology*, 99(10), 4044-4064.

10. Chiu, S.-F., Chiu, J.-Y., Kuo, W.-C. 2013. Biological stoichiometric analysis of nutrition and ammonia toxicity in thermophilic anaerobic co-digestion of organic substrates under different organic loading rates. *Renewable Energy*, 57(0), 323-329.

11. Desloover, J., De Vrieze, J., Van de Vijver, M., Mortelmans, J., Rozendal, R., Rabaey, K. 2014. Electrochemical nutrient recovery enables ammonia toxicity control and biogas desulfurization in anaerobic digestion. *Environmental Science & Technology*, 49(2), 948-955.

12. Hansen, K.H., Angelidaki, I., Ahring, B.K. 1998. Anaerobic digestion of swine manure: inhibition by ammonia. *Water Research*, 32(1), 5-12.

13. Hattori, S. 2008. Syntrophic acetate-oxidizing microbes in methanogenic environments. *Microbes and Environment*, 23(2), 118-27.

14. Hejnfelt, A., Angelidaki, I. 2009. Anaerobic digestion of slaughterhouse by-products. *Biomass and Bioenergy*, 33(8), 1046-1054.

15. Kim, W., Shin, S., Cho, K., Han, G., Hwang, S. 2014. Population dynamics of methanogens and methane formation associated with different loading rates of organic acids along with ammonia: redundancy analysis. *Bioprocess and Biosystems Engineering*, 37(5), 977-981.

16. Laureni, M., Palatsi, J., Llovera, M., Bonmatí, A. 2013. Influence of pig slurry characteristics on ammonia stripping efficiencies and quality of the recovered ammonium-sulfate solution. *Journal of Chemical Technology & Biotechnology*, 88(9), 1654-1662.

17. Morris, R., Schauer-Gimenez, A., Bhattad, U., Kearney, C., Struble, C.A., Zitomer, D., Maki, J.S. 2013. Methyl coenzyme M reductase (mcrA) gene abundance correlates with activity measurements of methanogenic H2/CO2-enriched anaerobic biomass. *Microbial Biotechnology*, 7(1), 77-84.

18. Niu, Q., Qiao, W., Qiang, H., Li, Y.-Y. 2013. Microbial community shifts and biogas conversion computation during steady, inhibited and recovered stages of thermophilic methane fermentation on chicken manure with a wide variation of ammonia. *Bioresource Technology*, 146, 223-233.

19. Ripley, L.E., Boyle, W.C., Converse, J.C. 1986. Improved alkalimetric monitoring for anaerobic digestion of high-strength wastes. *Journal (Water Pollution Control Federation)*, 58(5), 406-411.

20. Schloss, P.D., Westcott, S.L., Ryabin, T., Hall, J.R., Hartmann, M., Hollister, E.B., Lesniewski, R.A., Oakley, B.B., Parks, D.H., Robinson, C.J., Sahl, J.W., Stres, B., Thallinger, G.G., Van Horn, D.J., Weber, C.F. 2009. Introducing mothur: open-source, platform-independent, community-supported software for describing and comparing microbial communities. *Applied and Environmental Microbiology*, 75(23), 7537-7541.

21. Sotres, A., Cerrillo, M., Viñas, M., Bonmatí, A. 2015a. Nitrogen recovery from pig slurry in a two-chambered bioelectrochemical system. *Bioresource Technology*, 194, 373-382.

22. Sotres, A., Díaz-Marcos, J., Guivernau, M., Illa, J., Magrí, A., Prenafeta-Boldú, F.X., Bonmatí, A., Viñas, M. 2015b. Microbial community dynamics in two-chambered microbial fuel cells: effect of different ion exchange membranes. *Journal of Chemical Technology & Biotechnology*, 90(8), 1497-1506.

23. Steinberg, L.M., Regan, J.M. 2009. mcrA-targeted real-time quantitative PCR method to examine methanogen communities. *Applied and Environmental Microbiology*, 75(13), 4435-4442.

24. Sundberg, C., Al-Soud, W.A., Larsson, M., Alm, E., Yekta, S.S., Svensson, B.H., Sorensen, S.J., Karlsson, A. 2013. 454 pyrosequencing analyses of bacterial and archaeal richness in 21 full-scale biogas digesters. *FEMS Microbiology Ecology*, 85(3), 612-26.

25. Tartakovsky, B., Mehta, P., Bourque, J.S., Guiot, S.R. 2011. Electrolysis-enhanced anaerobic digestion of wastewater. *Bioresource Technology*, 102(10), 5685-5691.

26. Tuan, N.N., Chang, Y.C., Yu, C.P., Huang, S.L. 2014. Multiple approaches to characterize the microbial community in a thermophilic anaerobic digester running on swine manure: a case study. *Microbiological Research*, 169(9-10), 717-24.

27. Wang, Q., Garrity, G.M., Tiedje, J.M., Cole, J.R. 2007. Naïve bayesian classifier for rapid assignment of rRNA sequences into the new bacterial taxonomy. *Applied and Environmental Microbiology*, 73(16), 5261-5267.

28. Wang, Y., Zhang, Y., Wang, J., Meng, L. 2009. Effects of volatile fatty acid concentrations on methane yield and methanogenic bacteria. *Biomass and Bioenergy*, 33(5), 848-853.

29. Weld, R.J., Singh, R. 2011. Functional stability of a hybrid anaerobic digester/microbial fuel cell system treating municipal wastewater. *Bioresource Technology*, 102(2), 842-847.

30. Yenigün, O., Demirel, B. 2013. Ammonia inhibition in anaerobic digestion: A review. *Process Biochemistry*, 48(5-6), 901-911.

31. Zhang, C., Yuan, Q., Lu, Y. 2014. Inhibitory effects of ammonia on methanogen mcrA transcripts in anaerobic digester sludge. *FEMS Microbiology Ecology*, 87(2), 368-77.

32. Zhang, Y., Angelidaki, I. 2015. Counteracting ammonia inhibition during anaerobic digestion by recovery using submersible microbial desalination cell. *Biotechnology and Bioengineering*, 112(7), 1478-1482.

33. Zhu, C., Zhang, J., Tang, Y., Zhengkai, X., Song, R. 2011. Diversity of methanogenic archaea in a biogas reactor fed with swine feces as the mono-substrate by mcrA analysis. *Microbiological Research*, 166(1), 27-35.

Tables

Table 1. Characterization of the diluted pig slurry used as feeding solution in the anaerobic digester (AD) in Phase 1 and Phases 2 to 5 (n=number of samples).

Parameter	Diluted pig slurry	
	Phase 1 (n=7)	**Phase 2 to 5** (n=16)
pH (-)	7.49±0.36	6.98±0.21
COD (g_{O2} kg^{-1})	31.34±3.77	63.36±6.30
NTK (g L^{-1})	1.76±0.03	3.69±0.26
$N\text{-}NH_4^+$ (g L^{-1})	1.23±0.11	2.64±0.25
TS (g kg^{-1})	17.58±0.73	34.70±2.65
VS (g kg^{-1})	12.35±0.69	23.87±1.88

Table 2. Operational conditions for the AD reactor and the MEC.

Phase	Period (d)	AD			MEC	
		OLR (kg_{COD} m^{-3} d^{-1})	NLR (kg_N m^{-3} d^{-1})	Recirculation (% feed flow rate)	OLR (kg_{COD} m^{-3} d^{-1})	NLR (kg_N m^{-3} d^{-1})
1	1 - 110	3.02±0.60	0.17±0.03	0	-	-
2	110 - 200	6.25±1.05	0.34±0.06	0	27.80±1.40	1.76±0.02
3	200 - 240			25	28.50±1.80	1.73±0.09
4	240 - 299			50	26.10±2.90	1.68±0.09
5	299 - 236			75	27.00±2.20	1.94±0.03

Table 3. Summary of the parameters for the AD and the MEC reactors in the different phases (n=number of samples). Results for the AD correspond to the stable period of each phase. n.a.; data not available as the stripping and absorption system was disconnected.

Parameter	Phase 1	Phase 2	Phase 3	Phase 4	Phase 5
AD					
n	9	5	4	5	6
CH_4 productivity (m^3_{CH4} m^{-3} d^{-1})	0.27±0.05	0.06±0.06	0.26±0.08	0.42±0.05	0.38±0.06
CH_4 (%)	74±1	67±1	66±1	67±2	66±1
Total alkalinity ($gCaCO_3$ L^{-1})	5.23±0.41	8.42±0.31	8.63±0.19	8.66±0.43	8.92±0.34
Partial alkalinity ($gCaCO_3$ L^{-1})	3.90±0.38	4.52±0.45	4.45±0.26	5.01±0.34	5.23±0.33
IA:TA	0.26±0.03	0.50±0.04	0.49±0.03	0.41±0.03	0.42±0.02
pH (-)	7.73±0.10	7.69±0.04	7.66±0.08	7.83±0.14	7.74±0.07
COD removal efficiency (%)	47±13	30±8	31±6	35±4	42±3
MEC					
n		14	11	14	10
COD removal efficiency (%)		25±8	28±7	30±11	20±7
$N\text{-}NH_4^+$ removal efficiency (%)		40±3	31±5	22±5	17±5
$N\text{-}NH_4^+$ absorbed (%)		30±6	13±3	n.a.	n.a
Current density (A m^{-2})		2.01±0.63	1.59±0.70	0.96±0.43	0.85±0.28
Anode pH (-)		7.03±0.07	7.47±0.19	7.64±0.25	7.56±0.07
Cathode pH (-)		11.83±0.60	12.02±0.25	11.67±0.27	11.66±0.17
AD-MEC					
COD removal efficiency (%)		46±5	51±7	59±7	56±7

Table 4. Diversity index for Eubacterial and Archaeal community of the MEC anode and AD effluent samples (mean±standard deviation). Data normalized to the sample with the lowest number of reads (16872 and 19235 for eubacterial and archaeal, respectively).

	Reads	**OTUs**	**Inverted Simpson**	**Shannon**
Eubacteria				
MEC_i	16872	706.00±0.00	17.50±0.00	4.27±0.00
MEC_f	22481	615.75±7.23	9.29±0.08	3.52±0.01
AD_{Phase1}	17776	489.51±2.98	15.44±0.04	3.58±0.00
AD_{Phase2}	20447	481.17±5.08	13.67±0.07	3.56±0.01
AD_{Phase3}	19778	474.51±4.95	8.03±0.05	3.21±0.01
AD_{Phase4}	20295	426.77±5.18	5.67±0.04	2.90±0.01
AD_{Phase5}	25178	520.70±7.21	12.70±0.10	3.51±0.01
Archaea				
MEC_i	56913	82.11±2.93	8.12±0.00	2.39±0.00
MEC_f	231636	26.96±0.26	1.01±0.00	0.05±0.00
AD_{Phase1}	19409	34.94±0.00	1.05±0.00	0.17±0.00
AD_{Phase2}	19235	37.00±1.47	1.06±0.00	0.20±0.01
AD_{Phase3}	25256	63.08±2.09	1.39±0.00	0.80±0.01
AD_{Phase4}	38734	35.99±0.66	1.21±0.00	0.45±0.00
AD_{Phase5}	20088	50.54±3.28	2.47±0.05	1.29±0.01

Figure captions

Figure 1 Scheme of the set up of the AD-MEC combined system coupled to the stripping and absorption unit.

Figure 2 Performance of the AD regarding (a) COD removal efficiency; (b) methane productivity; (c) IA:TA ratio; (d) VFA concentration; and (e) free ammonia concentration (FAN) and pH.

Figure 3 Performance of the MEC regarding (a) Current density; (b) ammonium removal efficiency; and (c) VFA concentration in the effluent.

Figure 4 Gene copy numbers for 16S rRNA and mcrA genes and ration between them, of the effluent of the AD at the five phases, and initial and final MEC anode biofilm (MECi and MECf, respectively).

Figure 5 Taxonomic assignment of sequencing reads from Eubacterial community of the effluent of the AD at the five phases, and initial and final MEC anode biofilm (MECi and MECf, respectively), at a) phylum b) family levels; and c) from Archaeal community at family level. Relative abundance was defined as the number of reads (sequences) affiliated with that taxon divided by the total number of reads per sample. Phylogenetic groups with relative abundance lower that 1% were categorized as “others”.

Figure 1

Click here to download Figure: Fig 1.eps

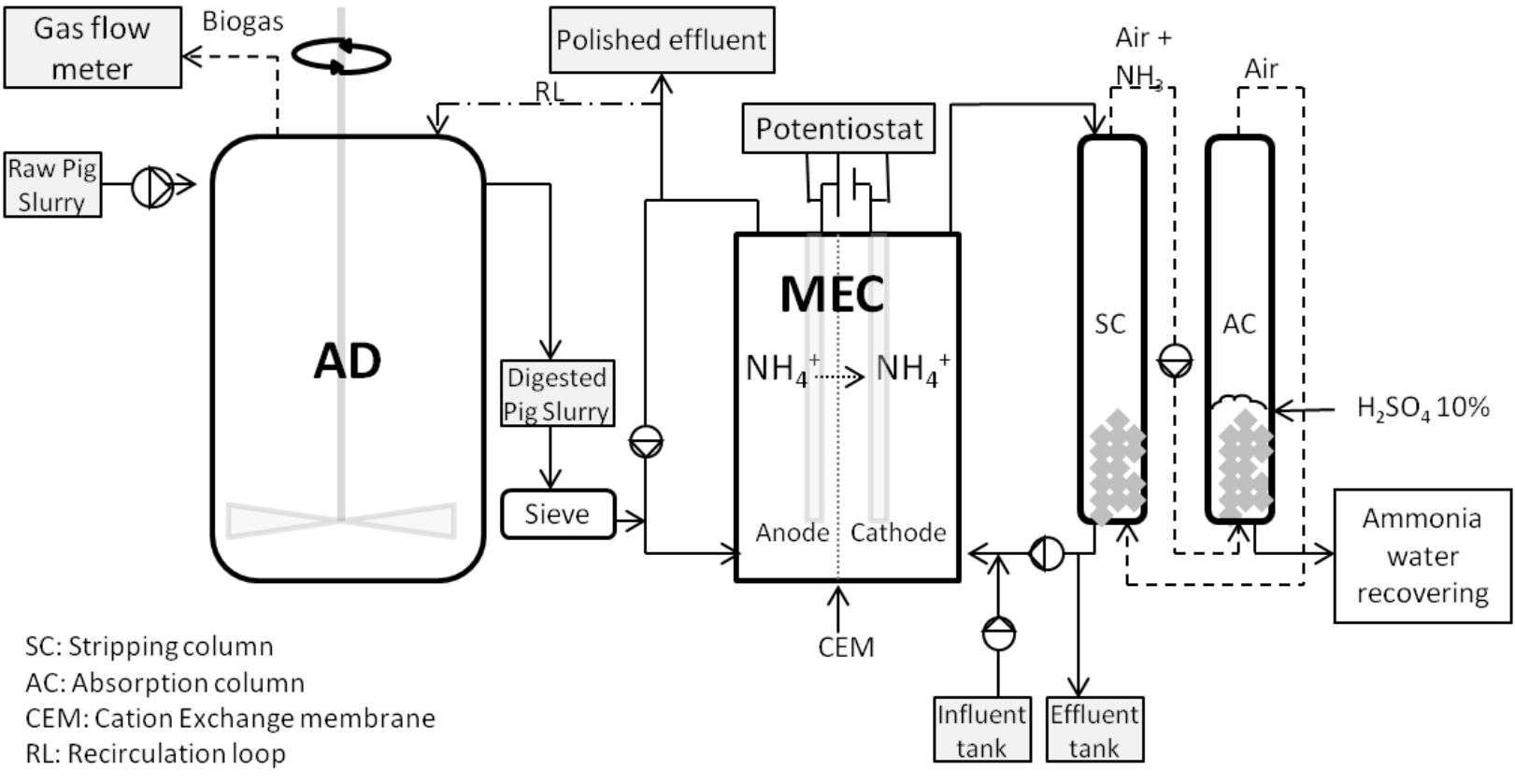

Figure 2

Click here to download Figure: Fig 2.eps

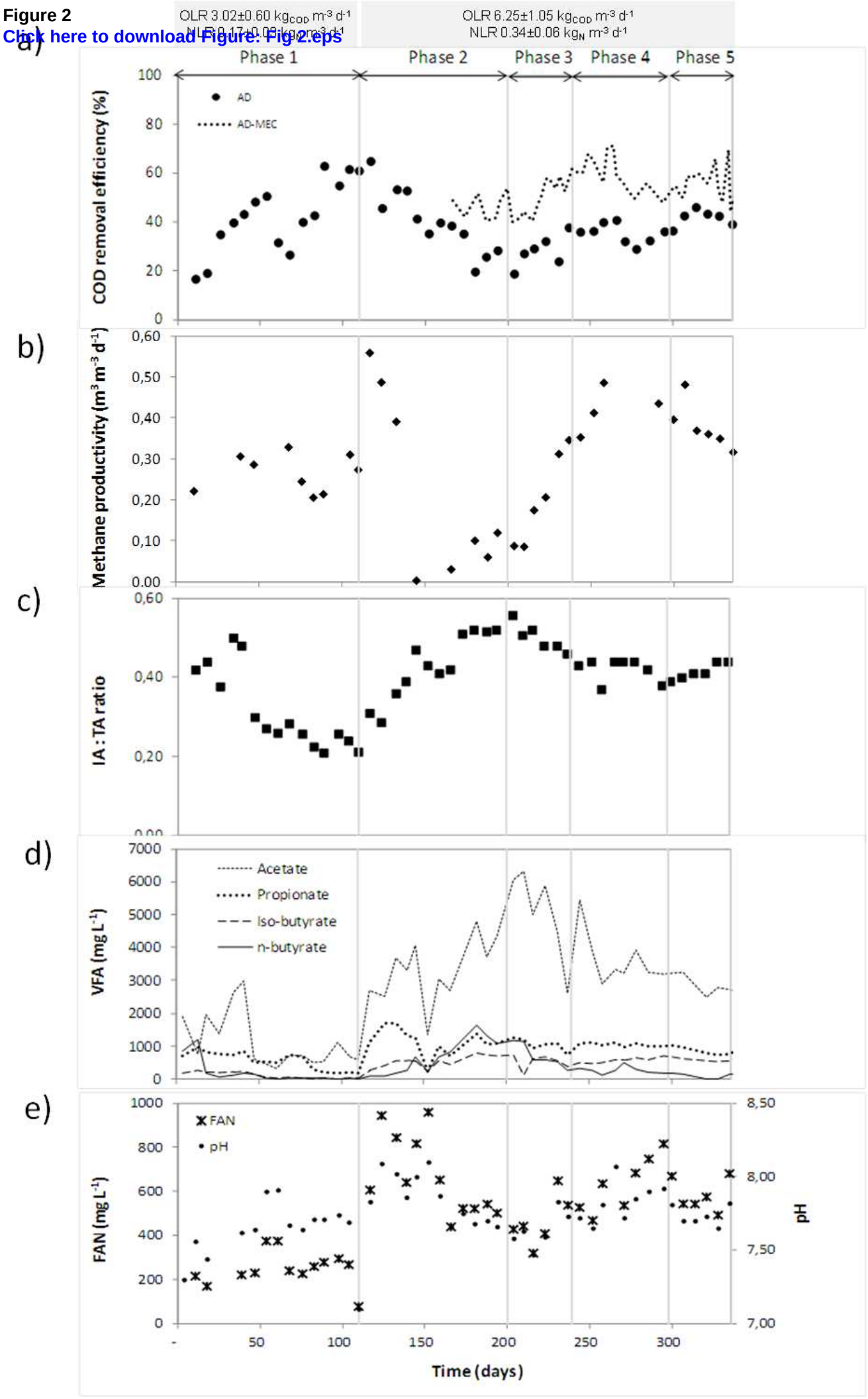

Figure 3
Click here to download Figure: Fig 3.eps

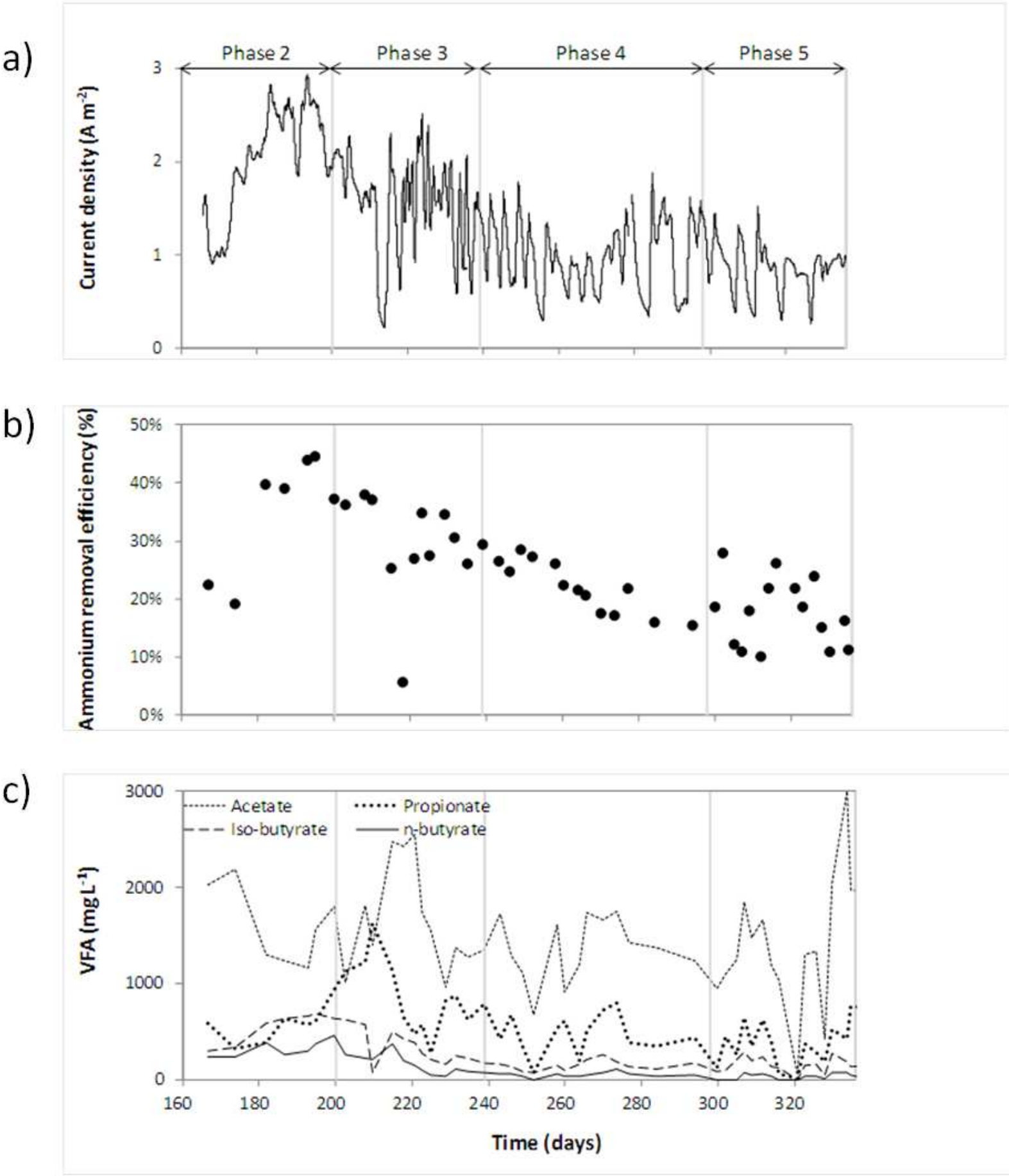

Figure 4

Click here to download Figure: Fig 4.eps

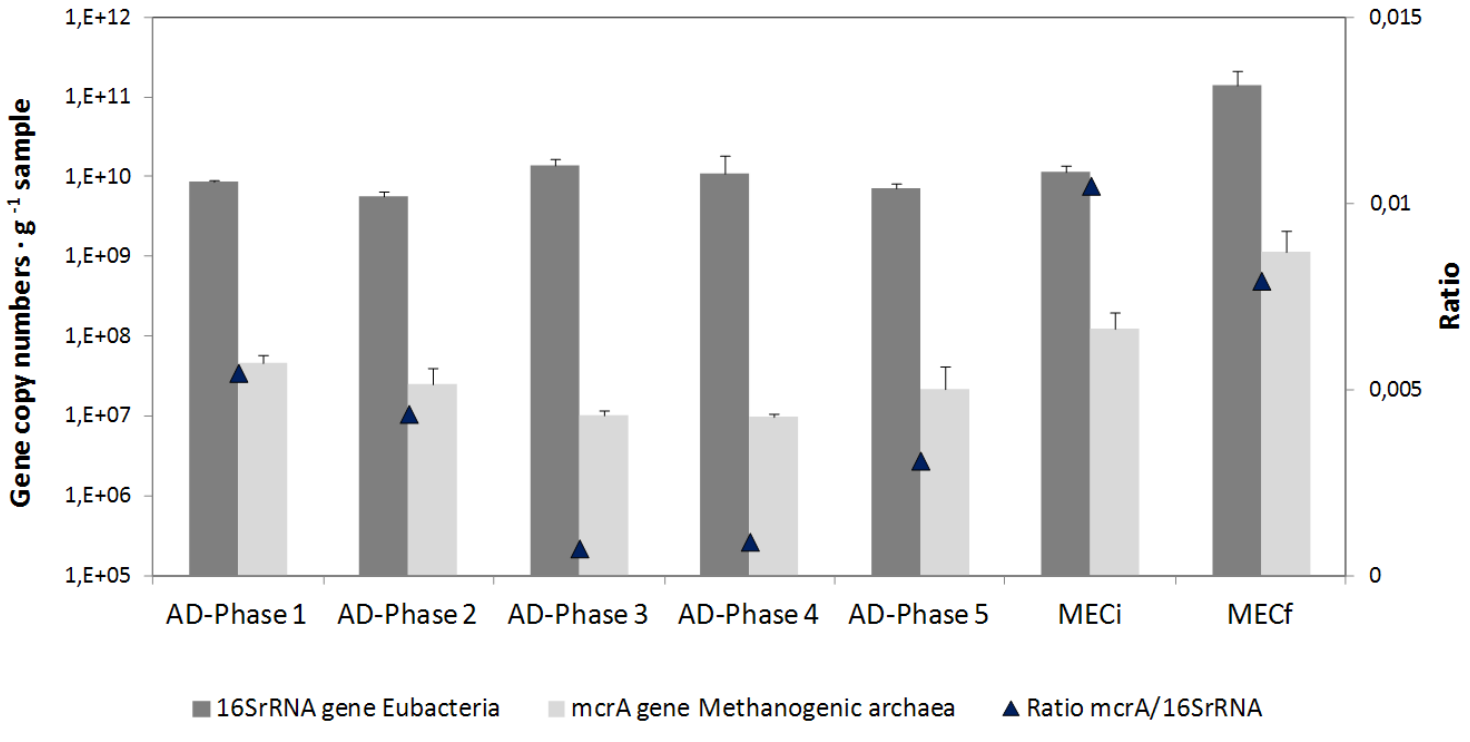

Figure 5

Click here to download Figure: Fig 5.eps